Geomechanics and Engineering, *Vol. 10, No. 6 (2016) 757-774*
DOI: http://dx.doi.org/10.12989/gae.2016.10.6.757

Finite element analysis of a CFRP reinforced retaining wall

Ahad Ouria [1a], Vahab Toufigh [*2], Chandrakant Desai [3b],
Vahid Toufigh [3c] and Hamid Saadatmanesh [4d]

[1] *Department of Civil Engineering, University of Mohaghegh Ardabili, Ardabil, Iran*
[2] *Department of Civil Engineering, Sharif University of Technology, Tehran, Iran*
[3] *Department of Civil Engineering, Graduate University of Advanced Technology, Kerman, Iran*
[4] *Department of Civil Engineering and Engineering Mechanics,*
University of Arizona, Tucson, AZ 85721-0072, USA

(*Received December 07, 2013, Revised June 19, 2015, Accepted March 01, 2016*)

Abstract. Soils are usually weak in tension therefore different materials such as geosynthetics are used to address this inadequacy. Worldwide annual consumption of geosynthetics is close to 1000 million m^2, and the value of these materials is probably close to US$1500 million. Since the total cost of the construction is at least four or five times the cost of the geosynthetic itself, the impact of these materials on civil engineering construction is very large indeed. Nevertheless, there are several significant problems associated with geosynthetics, such as creep, low modulus of elasticity, and susceptibility to aggressive environment. Carbon fiber reinforced polymer (CFRP) was introduced over two decades ago in the field of structural engineering that can also be used in geotechnical engineering. CFRP has all the benefits associated with geosynthetics and it boasts higher strength, higher modulus, no significant creep and reliability in aggressive environments. In this paper, the performance of a CFRP reinforced retaining wall is investigated using the finite element method. Since the characterization of behavior of soils and interfaces are vital for reliable prediction from the numerical model, soil and interface properties are obtained from comprehensive laboratory tests. Based on the laboratory results for CFRP, backfill soil, and interface data, the finite element model is used to study the behavior of a CFRP reinforced wall. The finite element model was verified based on the results of filed measurements for a reference wall. Then the reference wall simulated by CFRP reinforcements and the results. The results of this investigations showed that the safety factor of CFRP reinforced wall is more and its deformations is less than those for a retaining wall reinforced with ordinary geosynthetics while their construction costs are in similar range.

Keywords: CFRP; mechanically stabilized earth wall; finite element method; plasticity model

1. Introduction

Experiences have shown that earth materials have relatively good resistance against compression; however, they are weak in tension. Throughout history, several attempts have made

---

*Corresponding author, Assistant Professor, E-mail: toufigh@sharif.edu
[a] Assistant Professor
[b] Regents' Professor (Emeritus)
[c] Assistant Professor
[d] Professor

http://www.techno-press.org/?journal=gae&subpage=7 ISSN: 2005-307X (Print), 2092-6219 (Online)

to overcome the tensile weakness of soil to construct earth structures such as earth dams, slopes and retaining walls. Utilizing a tensile element within the soil mass to improve the tensile strength of the soil is a technique that has been used in the past. Today, using tensile elements in the soil mass is commonly used in earth structures such as Mechanically Stabilized Earth (MSE) wall that is developed in the current form since 1960. MSE wall structures are commonly used for retaining walls, bridge abutments, dams, seawalls, and dikes. Recently, MSE walls have become very popular mainly due to their flexibility, large bases, and cost effectiveness compared to conventional retaining walls.

The first MSE walls date to between 5000 B.C and 2500 B.C. The Babylonians constructed ziggurats (large towers) of earth that were reinforced with horizontal sheets of reed laid at regular intervals. The most notable remains of these ziggurats are those at Aqar Quf near Baghdad, Iraq. The overall height of the ziggurats was about 87 m (Retaining wall 2012). The first MSE wall in the United States was constructed in 1971 on State Route 39 near Los Angeles, California. Since 1997, approximately 23,000 MSE walls have been constructed in the world. The highest MSE wall built in the United States is 30 m (98 ft) high (Retaining wall 2012). At present, construction of mechanically stabilized earth (MSE) walls has increased significantly worldwide and specifically in the United States. For instance, on average more than 850 000 m^2 of MSE are constructed annually in the United States (Berg *et al*. 2009). The elements used for reinforcing can differ but they usually include steel and geosynthetics.

Vidal in 1960 introduced a technique in which galvanized steel strips were used in cohesionless soil to improve its properties. Since then, the use of geotextiles or synthetic fabrics as reinforcement has become more popular due to increased performance in comparison to metal reinforcement (Gray and Ohashi 1983). However, there are some significant problems associated with geotextiles, such as creep and low modulus of elasticity. In this study, Carbon Fiber Reinforced Polymer (CFRP) is used to address these problems. Due to the high tensile capacity of CFRP, which is one of the polymeric artificial products, numerous theoretical and experimental studies about their usage in reinforcing structures especially concrete have been performed. The results showed that CFRP is almost ten times stronger than steel in tension; therefore, it is possible to resolve the above issue by using CFRP as reinforcement in soil.

Saadatmanesh *et al*. (2010) studied the long-term behavior of different types of FRP laminates containing unidirectional and bidirectional fabrics such as carbon. The samples were exposed to nine different environments. These environments were simulated using four different chemical solutions with a pH of 12.5, 10, 7, and 2.5 and substitute seawater. Additional CFRP samples were exposed to ultraviolet (UV) radiation, temperatures of 60 and 50℃ (140 and 122℉) with 95% relative humidity (RH), and soil with 25% moisture content and active microorganisms in specially constructed chambers. Uniaxial tension tests were performed on the samples after 6000, 12,000, and 20,000 hours of exposure as well as on control samples; and tensile properties were measured for each specimen. The results showed the carbon laminates exhibited very little loss of mechanical properties under the above conditions.

In the first part of this research the properties of the carbon-FRP (CFRP) are found from tensile testing, and then interface properties between CFRP and a backfill soil are defined. After identifying the materials properties of CFRP, backfill soil, and interface, a solution procedure needs to be adopted. Limit equilibrium and the finite element methods are two among methods used commonly for analysis and design of reinforced soil structures.

Limit equilibrium is an easier approach that has been used to design reinforced soil structures. For initial design of MSE wall using CFRP, limit equilibrium method is used in this investigation.

Nevertheless, the limit equilibrium design approach does not account for deformations or stress distributions in soil or reinforcement (Rowe and Ho 1992). In addition, limit equilibrium methods often underestimated failure of two geosynthetics reinforced soil walls consisting of granular and cohesive backfills (Wu 1992).

Finite element analysis has been used widely in geotechnical problems and also to simulate the behavior of reinforced wall by Seed *et al*. (1986), Adib *et al*. (1990), Chew *et al*. (1990), Bathurst *et al*. (1992), Pal (1997), Fishman and Desai (1991) and El-Hoseiny (1999). It is has been realized that it is necessary to use appropriate constitutive models for soil, interface and reinforcement. A number of constitutive models have been used in finite element analysis. In this research, a hardening plasticity model is used for soil, Mohr-Column (M-C) model is used for interface, and linear elastic model is used for soil reinforcements and concrete panel.

2. Scope and objective

The objective of this paper involves testing and numerical model for soils and interface to simulate behavior of a MSE wall reinforced with CFRP, a novel reinforcement material. A comprehensive series of triaxial and interface shear tests were performed, then a numerical model was developed to model a MSE wall reinforced with CFRP by using Plaxis software. Finally, the results of the MSE wall reinforced with CFRP were compared with the MSE wall reinforced with geogrid.

3. Material modelling

3.1 Soil behavior

The Hardening soil (HS) model in Plaxis (2006) was used in numerical simulation of the CFRP reinforced retaining wall. Hardening soil model is based on two failure criteria and plastic potentials. A family of Mohr-Coulomb criterion for deviatoric failure and an elliptic cap for volumetric failure were used in HS model. Some properties of the HS model are described as follow:

- stress dependent stiffness according to a power law with input parameter m'
- Plastic straining due to primary deviatoric loading with input parameter E_{50}^{ref} .
- Plastic straining due to primary compression with input parameter E_{oed}^{ref} .
- Elastic unloading / reloading with input parameters E_{ur}^{ref} , v_{ur}.
- Failure according to the Mohr-Coulomb model with parameters c (cohesion), ϕ (internal friction angle) and ψ (dilatancy angle).

The basic idea for the formulation of the Hardening-Soil model is the hyperbolic stress-strain relationship. The stress dependent stiffness moduli for primary loading and unloading/reloading are defined as

$$\begin{aligned} E_{50} &= E_{50}^{ref}\ F(p) \\ E_{ur} &= E_{ur}^{ref}\ F(p) \end{aligned} \tag{1}$$

where

$$F(p) = \frac{c\cos\phi - \sigma'_3 \sin\phi}{\cos\phi + p^{ref}\sin\phi} \tag{2}$$

E_{50}^{ref} and E_{ur}^{ref} are the reference stiffness moduli in primary deviatoric loading and unloading reloading state corresponding to the reference stress p^{ref}.

E_{oed} is oedometric modulus and E_{oed}^{ref} is its value at reference stress of p^{ref} and is given by

$$E_{oed} = E_{oed}^{ref}\left(\frac{p}{p^{ref}}\right)^m \tag{3}$$

For the triaxial case the yield function is defined according to Eq. (4).

$$f = \frac{q_a}{E_{50}}\frac{q}{q_a - q} - \frac{2q}{E_{ur}} - \gamma^p \tag{4}$$

Where; q is deviatoric stress and q_a is equivalent to the shear strength.

The plastic shear strain γ^p according to Eq. (5) is used as the relevant parameter for frictional hardening.

$$\gamma^p = \varepsilon_1^p - \varepsilon_2^p - \varepsilon_3^p = 2\varepsilon_1^p - \varepsilon_v^p \approx 2\varepsilon_1^p \tag{5}$$

Where ε_{1p}, ε_{2p} and ε_{3p} are main components of plastic strain.

A cap type yield surface is introduced to close the elastic region in the direction of isotropic stress axis. The definition of the cap yield surface is as follow

$$f^c = \frac{q^2}{\alpha^2} + p^2 - p_p^2 \tag{6}$$

where α is the aspect ratio of the elliptic cap and p_p is the pre-compression pressure. Fig. 1 shows the shape of the yield surface in the principal stress space.

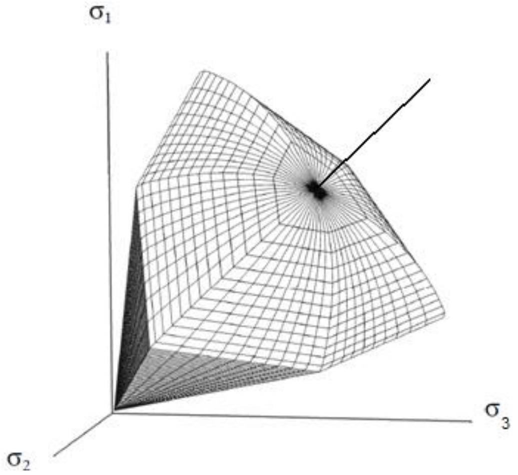

Fig. 1 Hardening-Soil model in principal stress space for cohesionless soil (Plaxis 2006)

The yield surface of a hardening plasticity model can expand due to plastic straining. Distinction is made between two main types of hardening, namely shear hardening and volumetric hardening. Shear hardening is used to model irreversible strains due to deviatoric loading. Compression hardening is used to model irreversible plastic strains due to compression in oedometer loading and isotropic loading (Schanz 1998). Further information about the Hardening model can be found in Plaxis material manual (Plaxis 2006).

3.1 Interface behavior

An elastic-plastic model was used to describe the behavior of the interfaces. The Mohr-Coulomb criterion is used to distinguish between elastic behavior, where small displacements can occur within the interface, and plastic interface behavior when permanent slip may occur.

For the interface to remain elastic the shear stress τ is given by

$$|\tau| < \sigma_n \tan\varphi_i + c_i \tag{7}$$

And for plastic behavior τ is given by

$$|\tau| = \sigma_n \tan\varphi_i + c_i \tag{8}$$

Where σ_n, φ_i and c_i are the normal stress, friction angle and cohesion of the interface respectively. The interface properties are calculated from the soil properties and a strength reduction factor, *R* can be used for interfaces.

$$\tan\varphi_i = R\ \tan\varphi_{soil} \leq \tan\varphi_{soil} \tag{9}$$

When the interface is elastic then both slipping (relative movement parallel to the interface) and gapping (relative displacements perpendicular to the interface) could be expected to occur. The magnitudes of these displacements are

$$\text{Elastic gap strain} = \frac{\sigma_{t_i}}{E_{oed,i}} t_i \tag{10}$$

$$\text{Elastic slip strain} = \frac{\tau t_i}{G_i} t_i \tag{11}$$

Where; σ_{ti} and τ_{ti} are normal and shear stress on the interface respectively, G_i is the shear modulus of the interface, $E_{oed,i}$ is the one-dimensional compression modulus of the interface and t_i is its thickness.

4. Materials and methods

4.1 Materials

4.1.1 Carbon fiber reinforced polymer

In this study, unidirectional carbon fabric was used with density of 779 g/m^2, and it was impregnated using Epoxy RL 200 to form the CFRP. Epoxy RL200 is used to transmit forces between fibers and the applied loads since adhesion between individual fibers is limited. Epoxy

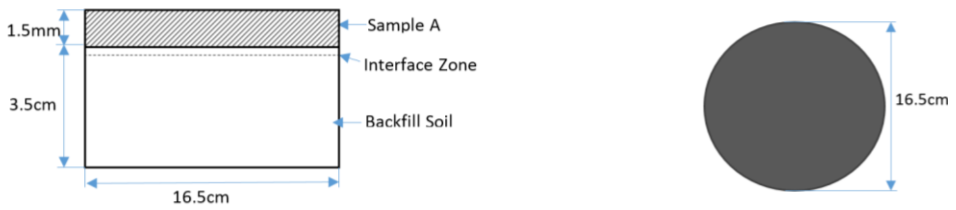

(a) (b)

Fig. 2 General over view of interface between soil and CFRP: (a) Configurations for interface layer for CFRP Sample & backfill; (b) CFRP sample

RL 200 is made of one part resin (bisphenol A based) and one part hardener (polyethylene polyamine) by volume. This epoxy has a pot life of 30 sec at room temperature and is fully cured after one hour at 25℃.

To obtain the material properties of CFRP, a total number of eight straight strips of CFRP with dimensions of 25.4 mm by 304.8 mm and thickness of 0.635 mm were tested in tension. The average tensile strength of 931 MPa, tensile modulus of elasticity of 60,949 MPa and Poisson's ratio of 0.34 were obtained from tests.

Note that HDPE geogrid (e.g., Tensar SR2), which is used for many soil-reinforcement projects such as Tanque Verde-Wrightstown-Pantano Roads project in Tucson, Arizona USA, has a maximum tensile strength of 17 MPa and tensile modulus of elasticity of 240 MPa. Based on these tests, the maximum tensile strength and tensile modulus of elasticity of Geo-Composite (CFRP) are approximately 50 and 250 times higher than maximum tensile strength and tensile modulus of elasticity of geogrid respectively.

4.1.2 Backfill soil

The soil was collected from Tanque Verde wash in Tucson, AZ USA. It is the same soil that Desai and El-Hoseiny (2005) reported for the MSE wall constructed near Tucson, AZ by using geogrid. The soil was classified as SP poorly graded or gravelly sand according to ASTM D2487-11. Followings are the index properties: specific gravity = 2.64; D10, D30, D60 = 0.48, 1.00, 1.75 mm, respectively; e_{max} = 0.71, e_{min} = 0.37; γd_{max} = 18.84 kN/m^3; γd_{min} = 15.35 kN/m^3; and optimum moisture content = 8.0%. The friction angle was 40 degrees which was determined by direct shear test according to ASTM D3080.

4.2 Methods

4.2.1 Sample preparation for interface testing

To fabricate a CFRP sample, a layer of carbon fiber with dimension of 20 × 20 cm was saturated by epoxy RL 200. The average thickness CFRP sample was approximately 1.5 mm. After complete curing the samples were cut in circular shape with diameter of slightly bigger than 16.5 cm for interface testing. Fig. 2 shows the details of the sample.

5. Experimental procedures and results

Three types of tests were performed: (1) triaxial tests on the backfill soil; (2) interface tests under displacement control on CFRP-Backfill; and (3) interface normal test under load control condition on CFRP-Backfill.

As it was mentioned previously, the same backfill soil was used in this investigation as Desai and El-Hoseiny (2005), who performed triaxial tests including loading, unloading, and reloading on the samples under different initial confining stresses, σ_3 = 17.5, 35.0, 52.0, 70.0, 140.0, 210.0, 345.0, and 420.0 kPa. The maximum confining pressure related to the approximate field pressure of about 480 kPa. Typical results for hydrostatic test and triaxial shear tests under σ_3 = 35, 210 and 420 kPa are shown in Fig. 3.

The interface and normal behavior between soil and the CFRP specimens were performed using CYMDOF (Cyclic Multi Degree of Freedom) device which is intended for testing the interfaces. Details of the CYMDOF device are given in Desai and Rigby (1997).

Cyclic shear tests were performed including loading, unloading, and reloading under a wide range of initial normal stresses such as 17.5 kPa, 35 kPa, 70 kPa, 140 kPa, 210 kPa, 350 kPa, 525 kPa, 875 kPa, and 1050 kPa. In these tests, vertical load was first applied on the specimen then horizontal (shear) load was applied by the displacement control method. Typical results for σ_n = 70, 210 and 875 kPa are shown in Fig. 4.

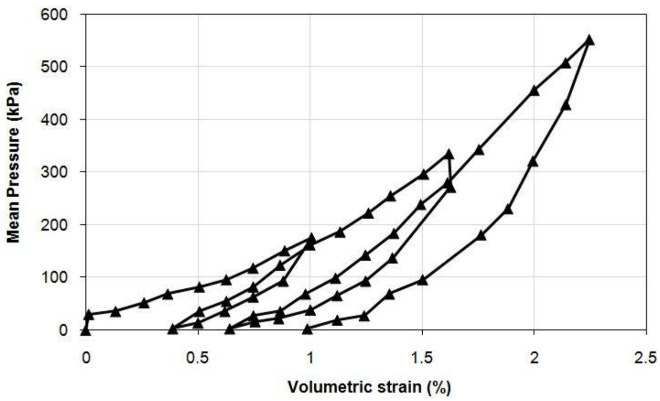

(a)

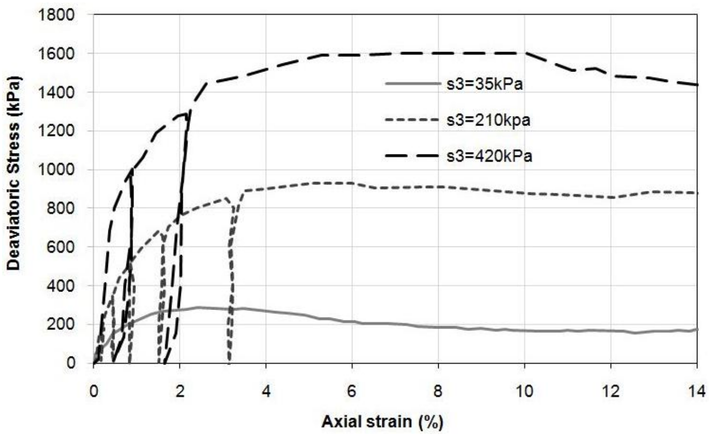

(b)

Fig. 3 Typical observed responses of soil for normal behavior and shear behavior for σ_3 = 35, 210 and 420 kPa (El-Hoseiny 1999)

The interface friction angle and adhesion between CFRP and soil were obtained as 41.5° and 58 kPa, respectively (Fig. 5).

Similar to the isotropic compression tests and cyclic shear tests, the normal tests on interface specimens were performed under a wide range of initial normal stresses to evaluate the normal stiffness of the interface. The results of the interface normal tests are shown in Fig. 6.

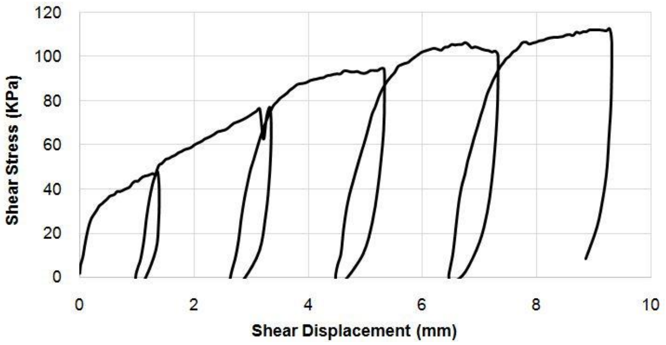

(a) Normal stress 70 KPa

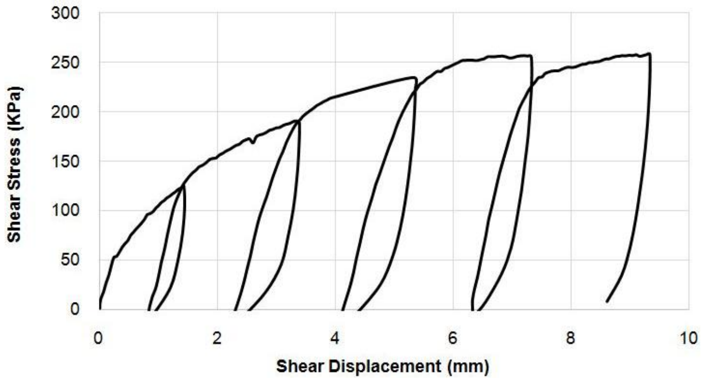

(b) Normal stress 210 KPa

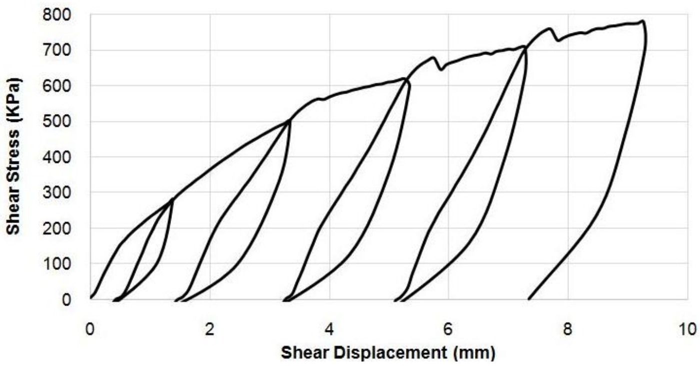

(c) Normal stress 875 KPa

Fig. 4 Direct shear interface result for CFRP-soil interfaces for: (a) normal stress = 70 kPa; (b) for initial normal stress = 210 kPa; (c) for initial normal stress = 875 kPa

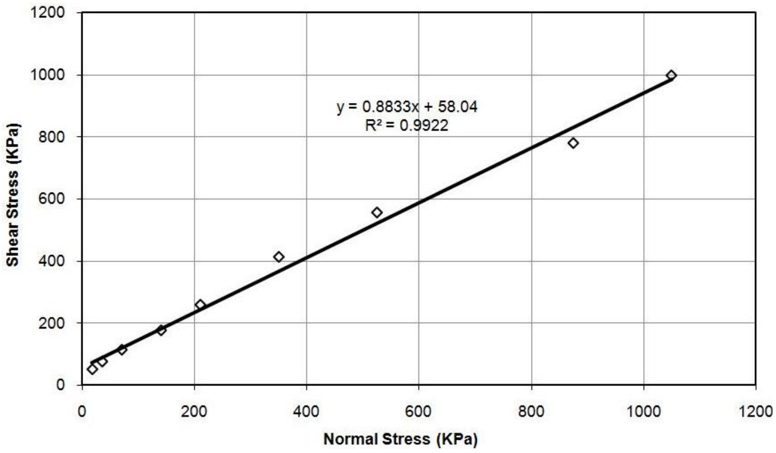

Fig. 5 Normal stress vs. max shear stress

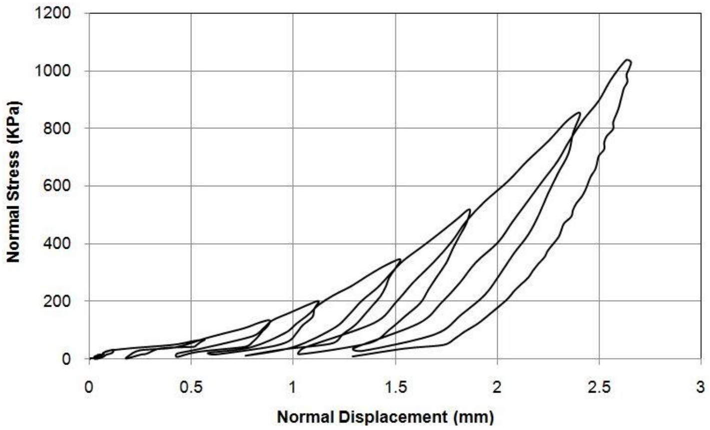

Fig. 6 Normal displacement vs. Induced normal stress

Interface shear and normal stiffness, k_s and k_n, were obtained as the average slopes of unloading and reloading curves shown in Figs. 4 and 5 respectively. However, as it was mentioned before, Plaxis (2006) assumes the strength properties of interfaces are linked to the strength properties of the soil layers by a strength reduction factor. Since the interface friction angle of the soil and CFRP was larger than friction angle of the soil, therefore the interface friction angle of soil and CFRP was assumed equal to the soil friction angle. This is one of the limitations of using the interface elements in Plaxis.

6. Finite element analysis

6.1 Numerical model

Plaxis program (2006) was used to simulate the MSE wall (Tanque Verde Wrightstown-Pantano Project, Panel 26-32). Hardening soil model was used to characterize the backfill soil and linear

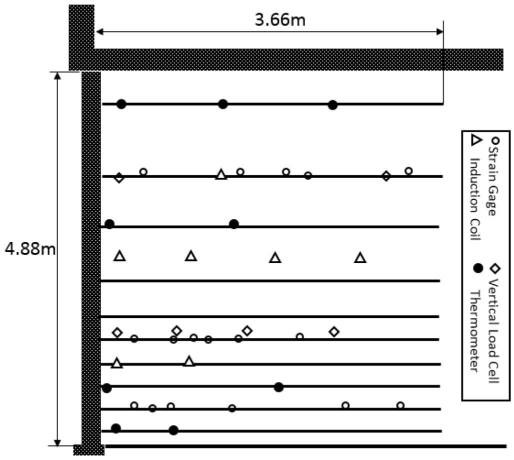

Fig. 7 Location of instruments for wall panel 26-32 (FHWA 1989)

elastic/plastic model was used for reinforcements and concrete panel, and Mohr-Coulomb model was used for interface.

6.2 Calibration the model

In order to calibrate the numerical model and examine its accuracy, the model was constructed based on an actual MSE wall as a reference model. The reference wall was instrumented with sensors at different depths of soil to provide the vertical stress, horizontal and vertical strains and temperatures (Desai and El Hoseiny 2005).

Forty three MSE walls unit were constructed at Tanque Verde Road to grade separated interchanges on the Tanque Verde Wrightstown-Pantano roads projects in Tucson, AZ, between November 1984 and October 1985. The project used geogrid geogrid reinforcement in mechanically stabilized earth (MSE) retaining walls in a large transportation related project in North America (FHWA 1989). The geometry of wall and the location of sensors in the reference wall are illustrated in Fig. 7.

Two panels, 26-30 and 26-32 were instrumented in the field. Panel 26-32 was simulated was used as the reference wall in this study. The wall height was 4.88 m and its width was 3 m made of precast reinforced concrete panel. Reinforced geogrids were connected to the concrete facing panels at the elevations shown in Fig. 7 and their length was 3.66 m. The geogrid was a uniaxial product made from high density polyethylene (HDPE) stabilized with about 2.5% carbon to provide resistance to attack by ultraviolet light (FHWA, 1989). At the top of the wall fill, a pavement structure composed of 10.2 cm coarse base covered by 24.1 cm of concrete was constructed. Further details of the configuration are given by Berg *et al*. (1986).

6.3 Parameters

Soil and interface parameters were determined from laboratory tests and reinforcement and concrete panel parameters were adopted from manufacturers' literature. The parameters used in numerical simulation were according to Table 1.

Table 1 Material parameters used in finite element analysis of MSE wall

(A) Parameters for backfill and interface

Material contant	Symbol	Backfill	Interface (geogrid)	Interface (CFRP)
Adhesion (kPa)	c	-	66	58
Friction angle/interface angle(degree)	ϕ/δ	40	34	41.5
Secant stiffness in standard drained triaxial test (MPa)	$E_{50}^{(\mathrm{ref})}$	42.8	-	-
Tangent stiffness for primary oedometer loading (MPa)	$E_{oed}^{(\mathrm{ref})}$	34.3	-	-
Unloading / reloading stiffness (MPa)	$E_{ur}^{(\mathrm{ref})}$	399.8	-	-
Power for Stress-level dependency of stiffness	m	0.5	-	-
Lateral coefficient (normal consolidation)	K_0^{nc}	0.4	-	-
Failure ratio	R_f	0.9	-	-
Reference stress for stiffnesses (kPa)	p^{ref}	100	-	-

(B) Parameters for geogrid and concrete wall

	Symbol	Geogrid	CFRP	Concrete panel
Axial stiffness (KN/m)	EA	2250.4	38703	-
Max axial tension force (KN/m)	N_p	19.0	591	-
Thickness (mm)	t	1.5	0.635	152.2
Tensile/compression modulus of elasticity (kPa)	E	1.50E+06	6.09E+07	2.10E+07
Poisson ratio	v	0.3	0.34	0.15

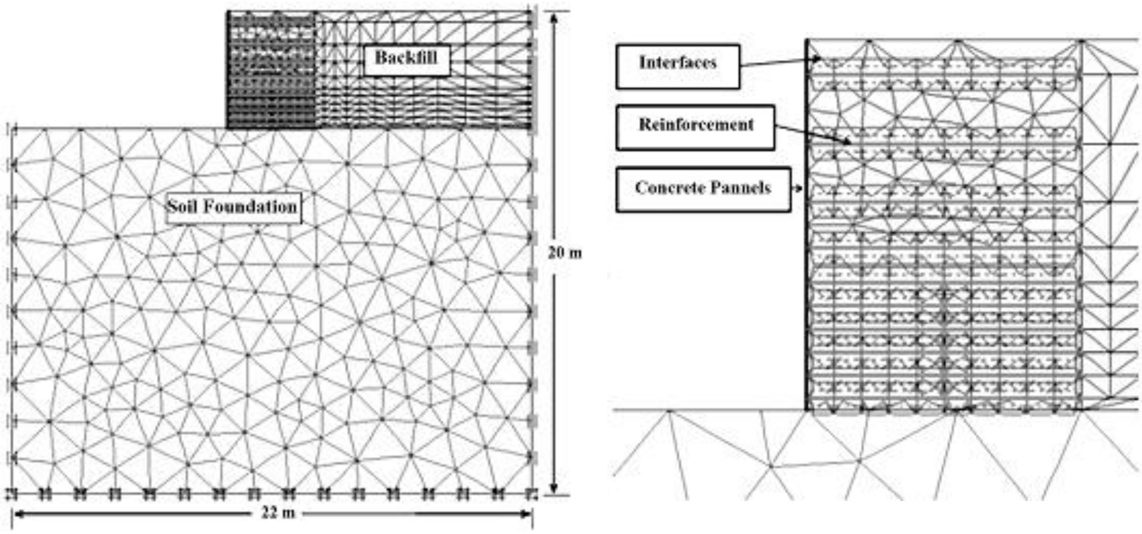

(a) Overall mesh (b) Mesh near geogrid

Fig. 8 Finite element mesh with interface elements

In the FE model the side boundaries were placed at a distance of 2.5 times of the length of the reinforcement and the bottom boundary was placed at a distance of about 3 times the height of the wall. Such distances and the assumed boundary conditions were considered to approximately simulate the semi-infinite extent of the system. Fig. 8 shows the details of the FE model.

Surcharge load including pavement and traffic loads was assumed to be equal to 20 kN/m (Desai and El-Hoseiny 2005). The rest of details for soil and wall facing of the configuration were the same as the one was investigated by Desai and El-Hoseiny (2005). The number of CFRP layers and their locations were designed to achieve internal and external safety factors similar to those in the reference wall.

6.4 Verification of the FE model

In order to verify the numerical model, the results of FE analysis were compared with the data obtained from the field (FHWA 1989). Vertical stress at the elevation of 1.5 m from the wall base

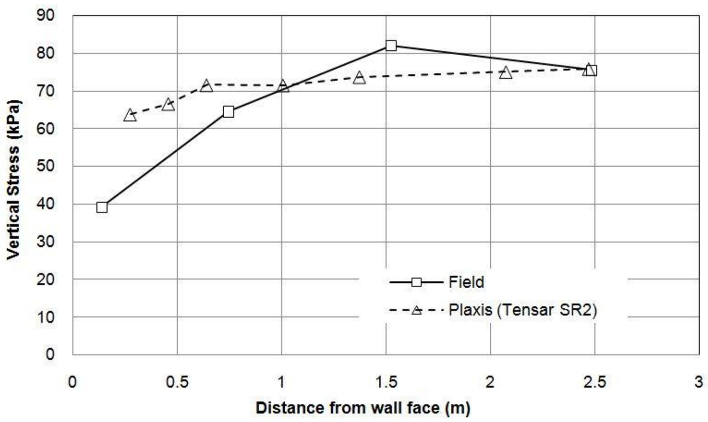

Fig. 9 Vertical stress vs. distance from the wall faces at elevation 1.5 m, after opening traffic

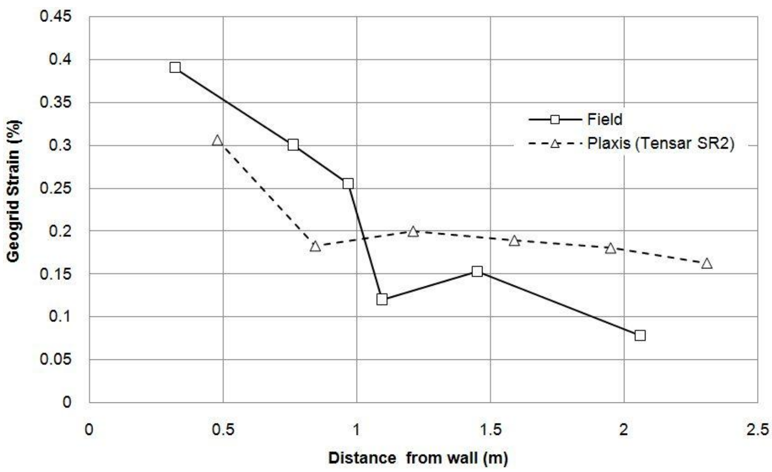

Fig. 10 Geogrid strain at elevation 1.4 m vs. distance from wall for panel 26-32 face at elevation 1.4 m, after opening traffic

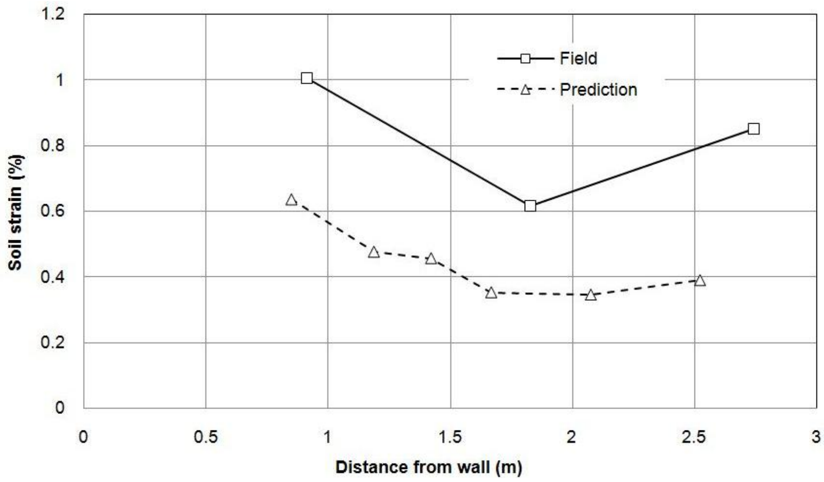

Fig. 11 Soil horizontal strain vs. distance from the wall at elevation 2.4 m, after opening traffic

resulted from numerical analysis are compared with vertical stress measured in the filed in Fig. 9.

Fig. 10 shows the axial strain in geogrid located at the elevation of 1.4 m from wall base. In this figure the data recorded by sensors in the field are shown. Horizontal strains of the soil at 2.4 m of the wall resulted from FE model and mustered in the field are shown in Fig. 11.

Based on these comparisons it can be concluded that the correlation between FE model and filed results are satisfactory. However, the comparison for soil somewhat is slightly different. The differences can be due to the sensors not perfectly installed, error in readings, and the limitations of model used in this study. However, it can be considered that the proposed model can be applicable for further analysis. Desai and El-Hoseiny (2005) used advanced DSC model and obtained satisfactory correlation and analyzed mainly Panel number 26-30. In the current analysis, a simpler model is used and Panel 26-32 is analyzed; however, the results are quite satisfactory.

7. Comparing MSE walls with CFRP and geogrid reinforcements

The application of CFRP in the reinforcement of retaining walls was study by comparing the performances of the reference wall reinforced by Geogrid and CFRP. Several configurations for number of reinforcements and their arrangements were studied using the calibrated numerical model. Fig. 12 shows some configurations used in this study.

The safety factor (SF) calculated for MSE wall reinforced with different layers of Geogrid and CFRP are shown in Fig. 13. Here SF and the displacement of the top of the wall for geogrid (10 layers) are shown by single values that the SF was calculated by the model and the displacement was taken from the field data.

Based on Fig. 13, the MSE wall reinforced with three number of CFRPs has factor of safety (SF) and maximum wall deformations at the top of the wall of 1.85 and 9 mm, respectively. On the other hand the MSE wall reinforced with ten numbers of geogrid has factor of safety and maximum wall displacement of 1.38 and 22 mm, respectively. Therefore, the MSE wall reinforced with three numbers of CFRP deforms less and is more stable than the MSE wall reinforced with ten layers of geogrid.

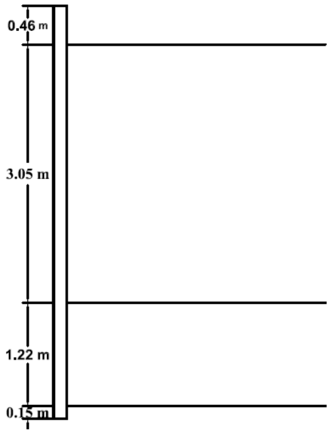

(a) Three CFRP reinforcement

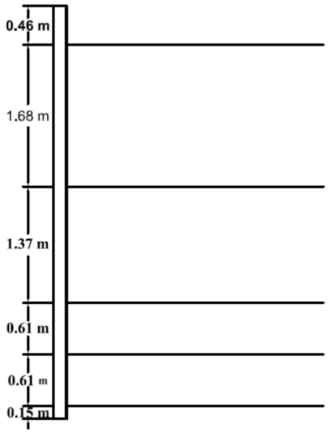

(b) Five CFRP reinforcement

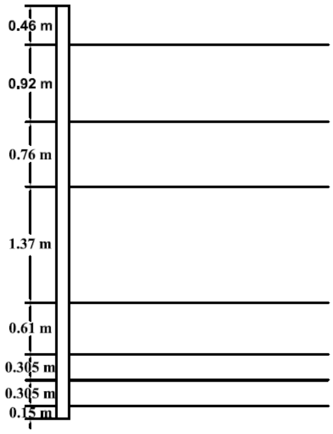

(c) Seven CFRP reinforcement

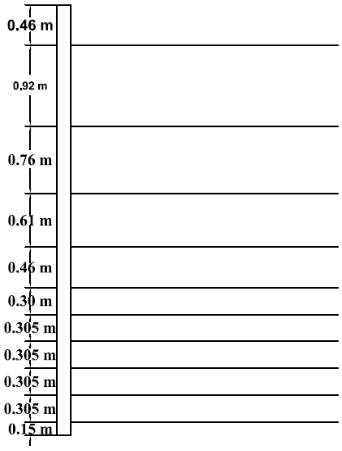

(d) Ten CFRP reinforcement

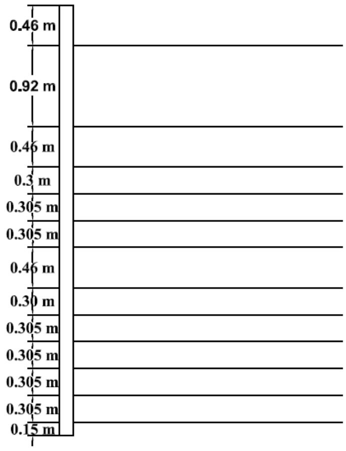

(e) Twelve CFRP reinforcement

Fig. 12 Location of CFRPs for different cases

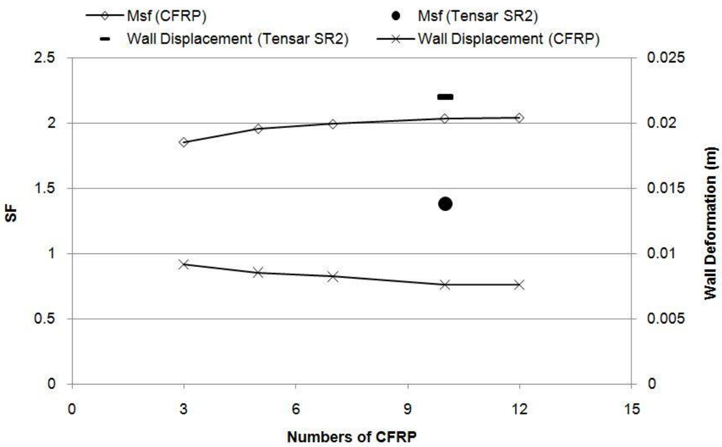

Fig. 13 Comparison of wall deformation and safety factor for different layers of CFRP Geogrid

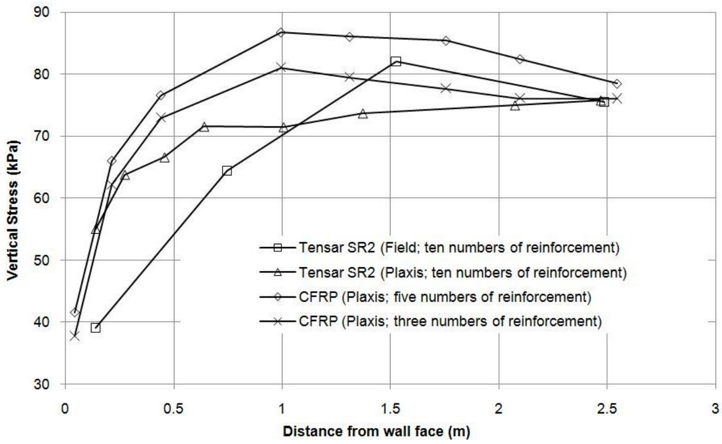

Fig. 14 Vertical stress vs. distance from wall face for CFRP and geogrid MSE wall at elevation 1.5 m

As shown in Fig. 13 as the number of CFRP increases the factor of safety increases and the maximum wall deformations decreases. For instance, the MSE wall reinforced with ten CFRPs has factor of safety and maximum wall deformation of 2.03 and 7.6 mm, respectively which has approximately 9 % higher factor of safety and 16% deform less than the MSE wall reinforced with ten numbers of CFRP. The MSE wall reinforced with three and five numbers of CFRPs were selected for further investigation.

Fig. 14 shows the vertical stress in the soil at the elevation of 1.5 m above the wall base and Fig. 15 shows the horizontal stress on wall face in different elevations. It can be seen in Fig. 14 that the vertical stress distribution in all cases is almost similar but CFRP shows higher vertical stress than geogrid. The horizontal stress for CFRP-wall is also higher than geogrid-wall as shown in Fig. 15. The results can be considered reasonable, since higher vertical stress is expected for higher horizontal stress. Note that field measurements for horizontal soil stress were not available for the adopted panel 26-32.

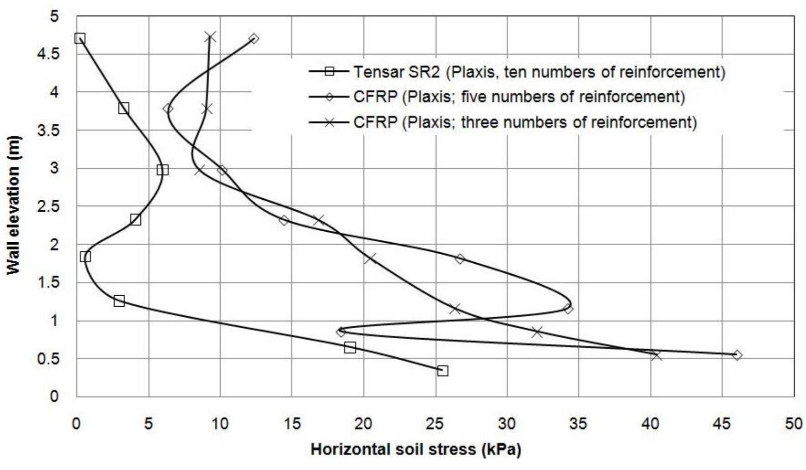

Fig. 15 Horizontal soil stress vs. elevation of the wall for CFRP and geogrid near wall face

Because of lower number of reinforcements, three or five, the stresses are higher in CFRP compared to that for ten layers of geogrid. This may not be of concern because the axial capacity of CFRP is much higher.

Fig. 16 shows axial forces in the reinforcements. It can be seen that the CFRP has tensile force higher than geogrid. In addition as numbers of CFRP decreases from five to three numbers of reinforcement, the values of vertical and horizontal stresses decrease (Figs. 14 and 15), and the tensile forces in reinforcement and wall movement decrease as expected (Figs. 16 and 17). To eliminate the vertical spacing limitation and for more stable wall, the MSE wall reinforced with five numbers of CFRP can be chosen for this case.

Computed horizontal displacements of the wall are illustrated in Fig. 17. As shown in this figure CFRP walls experiences movements much lower than geogrid wall. Since the stiffness of CFRP (*EA* where *E* = Young's elastic modulus and A is the area) is approximately 20 times higher than that of geogrid, the MSE wall with CFRP had approximately 15 mm smaller maximum

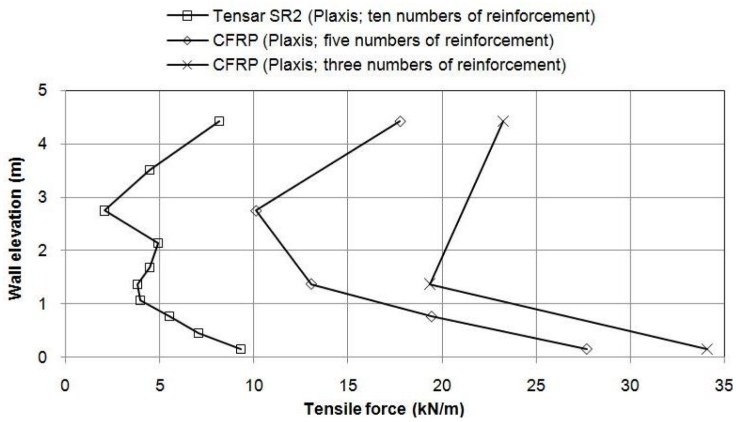

Fig. 16 Comparison of CFRP and geogrid for horizontal tensile force carried by reinforcement near wall face

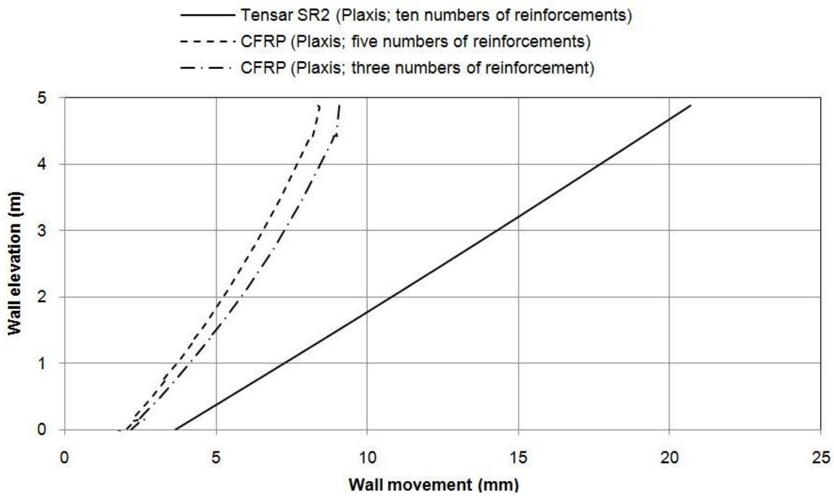

Fig. 17 Movement of the wall face for CFRP and geogrid MSE wall

horizontal deflection than the MSE wall with Tensar SR2. Based on the numerical results shown in Fig. 16 the factor of safety for tensile stress of CFRP in MSE wall was approximately 20; however, the factor of safety for geogrid in MSE wall was approximately 2.

8. Conclusions

In this study the applicability of CFRP in the reinforcement of retaining walls investigated using the finite element method. Material properties required for numerical simulations obtained from laboratory tests. The finite element model calibrated using the data available for a reference wall with Tensar geogrid. The geometry of the reference wall and its material properties were used in the numerical simulations. The results of the model for MSE wall reinforced with geogrid and CFRP were compared.

Based on the numerical results, the predicted displacements for CFRP were significantly lower than those for geogrid wall. This can be considered to be useful from design viewpoint. The safety factor was higher for five layers of CFRP wall than geogrid wall with ten layers.

The comparisons of costs for the two cases (ten layers of geogrid and five layers of CFRP) show that the costs for five layers of CFRP is slightly less than for ten numbers of geogrid. Considering the much higher strength and capacity of CFRP against environmental factors such as acidic environment (pH 2.5) CFRP would be more suitable. It loses approximately 10 % of its strength after 20,000 hrs while steel dissolves in this acidic environment. In an alkaline environment (pH 12.5) CFRPs approximately loses 5% of its strength after 20,000 hrs. On the other hand fiber glasses lose 60 % of its strength (Saadatmanesh *et al*. 2010). Thus, CFRP reinforcement can be considered as an alternative replacement for traditional geosynthetics from both strength and economic points of view.

Acknowledgments

We would like to thank Ed A. Farnaghi (Transportation Engineer; State of California, Department of Transportation, District 8) for helping in this research with cost analysis of ME walls.

References

Adib, M.E., Mitchell, J.K. and Christopher, B.R. (1990), “Finite element modeling of reinforced soil walls”, *Proceeding Design and Performance of Earth Retaining Structures,* ASCE Geotechnical Special Publication (P.C. Lamb and E. Hansen Eds.), No. 25, pp. 209-423.

ASTM D2487-11 (2011), Standard Practice for Classification of Soils for Engineering Purposes (Unified Soil Classification System), ASTM International, West Conshohocken, PA, USA.

ASTM D3080 (2004), Standard Test Method for Direct Shear Test of Soils under Consolidated Drained Conditions, Annual Book of ASTM Standards, ASTM International, West Conshohocken, PA, USA.

Bathurst, R.J., Karpurapu, R. and Jaret, P.M. (1992), “Finite element analysis of a geogrid reinforced soil wall”, *Proceeding Grouting, Soil Improvement and Geosynthetics, ASCE Geotechnical Special Publication* (R.H. Botden, R.D. Hohz and I. Juran Eds.), **30**(2), 1213-1224.

Berg, R.R., Bonaparte, R., Anderson, R.P. and Chouery, V.E. (1986), “Design, construction, and performance of two reinforced soil retaining walls”, *Proceedings of the 3rd International Conference on*

Geotextile, Vienna, Austria, April, Volume 2, pp. 401-406.

Berg, R.R., Christopher, B.R. and Samtani, N.C. (2009), "Design and construction of mechanically stabilized earth walls and reinforced soil slopes", U.S. Department of Transportation Federal Highway Administration, Vols. 1 & 2; Publication No. FHWA-NHI-10-024.

Budhu, M. (2008), *Foundations and Earth Retaining Structures*, John Wiley & Sons, NY, USA.

Chew, S.H., Schmertman, G.R. and Mitchell, J.K. (1990), "Reinforced soil wall deformations by finite element method", *Proceeding International Reinforced Soil Conference - Performance of Reinforced Soil Structures* (K.Z. Andrawes and A. McGown Eds.), Thomas Telford, Glasgow, Scotland, September, pp. 34-40.

Desai, C.S. and El-Hoseiny, K.E. (2005), "Prediction of field behavior of reinforced soil wall using advanced constitutive model", *J. Geotech. Geoenviron. Eng.*, **131**(6), 729-739.

Desai, C.S. and Rigby, D.B. (1997), "Cyclic interface and joint shear device including pore pressure effects", *J. Geotech. Geoenviron. Eng.*, **123**(6), 568-579.

El-Hoseiny, K.E. (1999), "Analysis of field Tensar retained wall with DSC model and FEM", Ph.D. Dissertation; Department of Civil Engineering and Engineering Mechanics, University of Arizona, Tucson, AZ, USA.

Federal Highway Administration (FHWA) (1989), Tensar geogrid-reinforced soil wall, Experimental Project No. 1; Ground Modification Systems, FHWA-EP-90-001-005, Washington, D.C., USA.

Fishman, K.L. and Desai, C.S. (1991), "Response of a geogrid earth reinforced retaining wall with full height precast concrete facing", *Proceedings Geosynthetics 91*, Atlanta, GA, USA, February, pp. 691-700.

Gray, D.H. and Ohashi, H. (1983), "Mechanics of bar reinforcement in sand", *J. Geotech. Eng. ASCE*, **109**(3), 335-353.

Janbu, J. (1963), "Soil compressibility as determined by Oedometer and Triaxial test", *Proceeding ECSMFE Wiesbaden*, Volume 1, pp. 19-25.

Pal, S. (1997), "Numerical simulation of geosynthetic reinforced earth structures using finite element method", Ph.D. Dissertation; Louisiana State University, Baton Rouge, LA, USA.

PLAXIAS b v (2006), Plaxis V8 manual, PLAXIAS b. v, Delft, Netherland.

Retaining Wall (2012), Wikipedia, Retrieved: March 21, 2012 3:06:10 PM. See: http://en.wikipedia.org/wiki/Retaining_wall

Rowe, R.K. and Ho, S.K. (1992), "A review of the behavior of reinforced soil walls", Preprint, Special and Keynote Lecture; *Proceedings of the International Symposium on Earth Reinforcement Practice*, (A.A. Balkema and Rotterdam), pp. 47-76.

Saadatmanesh, H., Tavakkolizadeh, M. and Mostofinejad, D. (2010), "Environmental effects on mechanical properties of wet lay-up fiber-reinforced polymer", *ACI Mater. J.*, **107**(3), 267-274.

Schanz, T. (1998), "Zur Modellierung des mechanischen verhaltens von reibungsmaterialen, habilitation" Stuttgart Universitat, Stuttgart, Germany.

Seed, R.B., Collin, J.G. and Mitchell, J.K. (1986), "FEM analysis of compacted reinforced soil walls", *Proceedings of the 2nd International Conference on Numerical Models in Geomechanics*, (G.N. Pande, W.F. Van Impe, E.M. Jackson and Son Publisher Redruth), Cornwall, England, March-April, pp. 553-562.

Toufigh, V. (2012), "Experimental and analytical studies of Geo-Composite applications in soil reinforcement", Ph.D. Dissertation; Department of Civil Engineering and Engineering Mechanics, University of Arizona, Tucson, AZ, USA.

Vidal, H. (1960), "The development and future of reinforced earth", Keynote Address; *Symposium on Earth Reinforcement, ASCE Annual Convention*, Pittsburgh, PA, USA, April.

Wu, J.T.H. (1992), "Predicting performance of the Denver walls: General reported", In: *Geosynthetic–Reinforced Soil Retaining Walls*, A.A. Balkema, pp. 3-20.

JS